

Kondo screening and exhaustion in the periodic Anderson model

D. Meyer* and W. Nolting

Lehrstuhl Festkörpertheorie, Institut für Physik, Humboldt-Universität zu Berlin, Invalidenstr. 110, 10115 Berlin

We investigate the paramagnetic periodic Anderson model using the dynamical mean-field theory in combination with the modified perturbation theory which interpolates between the weak and strong coupling limits. For the symmetric PAM, the ground state is always a singlet state. However, as function of the hybridization strength, a crossover from collective to local Kondo screening is found. Reducing the number of conduction electrons, the local Kondo singlets remain stable. The unpaired f -electrons dominate the physics of the system. For very low conduction electron densities, a large increase of the effective mass of the quasiparticles is visible, which is interpreted as the approach of the Mott-Hubbard transition.

I. INTRODUCTION

The periodic Anderson model (PAM) is one of the standard models for heavy fermion systems¹. In its simplest form, it describes a system of localized electronic states which hybridize with an uncorrelated conduction band. Except for a few statements concerning ground state properties², no exact solution of the PAM is known up to now. There have been many approximate calculations like QMC^{3,4,5,6,7,8,9}, perturbation theory^{10,11,12} as well as other analytical approaches^{13,14,15,16,17,18,19,20,21,22,23}. However, it is still far from being understood. Closely related to the PAM is the single-impurity Anderson model (SIAM)¹. The SIAM is one of the best-understood models in theoretical physics; besides a broad range of approximate solutions even some exact calculations are possible (for a detailed review, see reference 1). The main result of these calculations is the emergence of a new temperature scale T_K (*Kondo Temperature*), which governs the low-temperature physics. For $T < T_K$, the magnetic moment of the impurity is screened by conduction electrons (*Kondo screening*). All thermodynamic properties can be expressed in terms of T_K .

However, due to the periodicity of the localized states in the case of the PAM, new and more complicated physical properties will emerge. The most prominent example is the so-called exhaustion problem first mentioned by Nozières²⁴. His argumentation was based on the Kondo lattice model (KLM), which can be derived from the PAM under the condition of half-filling for the localized states using the Schrieffer-Wolff transformation^{1,25}. In the KLM, where the charge degrees of freedom of the localized states have been removed, Kondo screening manifests itself in the quenching of the magnetic moment of the localized spins by the conduction electrons. Reducing the number of conduction electrons below half-filling, however, the situation changes. The conduction band occupation is not sufficient to screen the localized spins completely. The nature of the ground state is not clear. As noted by Nozières²⁴, the situation is different for the case of small and large J , respectively. Whereas for small J , the screening is a collective effect, in the limit $J \rightarrow \infty$, it can be understood as the formation of local Kondo singlets, in which one conduction electron and one $S = \frac{1}{2}$ -

spin form a bound singlet state. On removing conduction electrons, some of these local Kondo singlets (LKS) will be broken. The remaining “bachelor” spins can be described as a system of hard-core fermions, for which double occupancy is forbidden²⁴. The small- J limit with its collective screening is more complicated. But nevertheless, following Nozières, this case can similarly be mapped onto an effective Hubbard model²⁴.

Contrary to the above-described KLM, the localized states also have a charge degree of freedom in the PAM, and its physical properties are therefore more complicated. The Schrieffer-Wolff transformation is valid only in the small $J = \frac{V^2}{U}$ -limit (V is the hybridization strength between localized and the conduction band states and U is the on-site Coulomb interaction among the localized electrons (see section II)). So, especially in the limit of strong hybridization between localized and conduction states, the KLM is not *a priori* justified as an effective model for the PAM. For the weakly hybridized case, the exhaustion in the PAM has recently been discussed by several authors^{4,5,19,20}. They find that Nozières’ picture of the effective Hubbard model also holds in this case and explains the emergence of a new low-temperature scale.

In this paper, we want to present a systematic investigation of the PAM. In the following chapter, we will introduce the theoretical approach, which combines the dynamical mean-field theory (DMFT)^{26,27,28} with a modification of the iterated perturbation theory (IPT)^{29,30,31,32}. The results will be presented in section III. In the first part of the discussion, we will focus on the hybridization-strength dependence of the symmetric PAM, and in the second part, we reduce the number of conduction electrons and investigate the exhaustion problem, thereby extending the discussion of reference 19.

II. THEORY

The PAM is defined by its Hamiltonian

$$H = \sum_{\vec{k}, \sigma} \epsilon(\vec{k}) s_{\vec{k}, \sigma}^\dagger s_{\vec{k}, \sigma} + \sum_{i, \sigma} e_f f_{i, \sigma}^\dagger f_{i, \sigma} + V \sum_{i, \sigma} (f_{i, \sigma}^\dagger s_{i, \sigma} + s_{i, \sigma}^\dagger f_{i, \sigma}) + \frac{1}{2} U \sum_{i, \sigma} n_{i, \sigma}^{(f)} n_{i, -\sigma}^{(f)} \quad (1)$$

with $s_{i, \sigma}$ ($f_{i, \sigma}$) and $s_{i, \sigma}^\dagger$ ($f_{i, \sigma}^\dagger$) being the conduction band (f -level) electron annihilation and creation operators ($n_{i, \sigma}^{(f)} = f_{i, \sigma}^\dagger f_{i, \sigma}$). $\epsilon(\vec{k})$ is the dispersion of a non-degenerate s -type conduction band and e_f denotes the position of the f -level with respect to the center of gravity of the conduction band. The hybridization V is taken as a \vec{k} -independent constant, and finally U is the local Coulomb interaction between two f -electrons at the same lattice site.

To obtain the the f -electron Green function $G_{ii\sigma}^{(f)}(E) = \langle\langle f_{i\sigma}; f_{i\sigma}^\dagger \rangle\rangle$, we apply a two-step procedure. The first of these, known as *dynamical mean-field theory* (DMFT)^{26,27,28}, is a mapping of the PAM onto a simpler model, namely the single-impurity Anderson model. The second step of our procedure is to find an approximate solution of the SIAM using the modified perturbation theory (MPT)^{30,31,32}.

The starting point of the DMFT is the assumption of a \vec{k} -independent, i.e. local self-energy $\Sigma_\sigma(E)$. It can be shown that in this case, the self-energy of the PAM is equivalent to the self-energy of a properly defined impurity model (SIAM). The conduction band within this SIAM has to be determined by the following expression for the hybridization function¹

$$\Delta_\sigma(E) = E - e_f - \Sigma_\sigma(E) - \left(G_{ii\sigma}^{(f)}(E)\right)^{-1} \quad (2)$$

In the original SIAM, this function is given as $\Delta(E) = \sum_{\vec{k}} \frac{V^2}{E - \epsilon(\vec{k})}$. All information of the conduction band and its hybridization with the impurity is contained in $\Delta(E)$. Therefore its knowledge is sufficient to define the electron bath of the SIAM also within the DMFT.

From the self-energy $\Sigma_\sigma(E)$ of the SIAM defined by $\Delta_\sigma(E)$, the PAM f -electron Green function can directly be obtained as

$$G_{ii\sigma}^{(f)}(E) = \frac{1}{N} \sum_{\vec{k}} \frac{1}{E - e_f - \frac{V^2}{E - \epsilon(\vec{k})} - \Sigma_\sigma(E)} \quad (3)$$

Since $G_{ii\sigma}^{(f)}(E)$ enters expression (2), a self-consistent solution has to be found by iteration. As already noted above, the DMFT-procedure becomes exact for a local, i. e. \vec{k} -independent self-energy. It has been shown that for the limit of infinite dimensions, or equivalently in the limit of the lattice coordination number going to infinity, this is indeed exactly the case^{26,33}. Furthermore,

solving the PAM in three dimensions using perturbation theory, it was shown that the results obtained in the local approximation compare qualitatively and quantitatively very well with those where the full \vec{k} -dependence has been considered^{11,34}.

Now the actual problem is shifted to solve the SIAM which is defined by $\Delta_\sigma(E)$ (see equation (2)). For this task we apply the modified perturbation theory (MPT)^{30,31,32} which is based on the following ansatz for the electronic self-energy^{29,35}

$$\Sigma_\sigma(E) = U \langle n_{-\sigma}^{(f)} \rangle + \frac{a_\sigma \Sigma_\sigma^{(\text{SOC})}(E)}{1 - b_\sigma \Sigma_\sigma^{(\text{SOC})}(E)} \quad (4)$$

where $\Sigma_\sigma^{(\text{SOC})}(E)$ denotes the second-order contribution to the second-order perturbation theory around the Hartree-Fock solution (SOPT-HF)^{11,36,37}. Please note that the ansatz (4) is \vec{k} -independent by construction, the basic assumption of the DMFT procedure is therefore already incorporated. Hence, the ansatz (4) together with the proposal to fit the parameters as will be described in detail below is the only approximation necessary to obtain the f -electron Green function.

The coefficients a_σ and b_σ are determined so that the first four ($n \in \{0, 1, 2, 3\}$) moment sum rules

$$M_\sigma^{(n)} = \int dE E^n A_\sigma^{(f)}(E) = \langle \underbrace{[[\dots [f_\sigma, H]_-, \dots, H]_-, f_\sigma^\dagger]_+}_{n\text{-fold commutator}} \rangle \quad (5)$$

$$A_\sigma^{(f)}(E) = -\frac{1}{\pi} \Im G_{ii\sigma}^{(f)}(E + i0^+)$$

are fulfilled^{30,38}. $\Im x$ denotes the imaginary part of x .

Since the moments $M_\sigma^{(n)}$ determine the high-energy expansion of the Green function, the compliance of the $n = 3$ sum rule automatically leads to the correct behavior of $G_{ii\sigma}^{(f)}(E)$ up to the order $\frac{1}{E^4}$ ³⁸. Furthermore, the $n = 3$ sum rule is directly related to the correct positions and spectral weights of the charge excitations in the strong-coupling limit $U \rightarrow \infty$ ^{38,39}. This is ensured by the occurrence of a higher-order correlation function called bandshift B_σ , which is discussed in detail in the context of the Hubbard model in reference 38, and in reference 30 for the effective SIAM within the dynamical mean-field theory.

Since we use the perturbation theory around the Hartree-Fock solution to determine the $\Sigma_\sigma^{(\text{SOC})}(E)$, another parameter enters the calculation, namely the chemical potential within the Hartree-Fock calculation. It is *a priori* not evident that this chemical potential should be identical to the chemical potential of the full problem. In fact, several other choices to determine this parameter seem possible. Within the iterated perturbation theory (IPT)^{19,29}, which is away from half-filling also based on the ansatz (4), the Luttinger sum⁴⁰ or equivalently the Friedel sum rule^{41,42} is used. This, however, limits the

calculation to $T = 0$ from the very beginning. We therefore define a different constraint, demanding that the impurity occupation number within the Hartree-Fock calculation is equivalent to the true occupation number. A detailed investigation of this choice and other possibilities is found in reference 30. Investigating the well-known single-impurity Anderson model to test the quality of our method³², we found that the MPT fulfills the Friedel sum rule within numerical accuracy not only under symmetric parameter conditions but also in a broad range of parameters, especially when reducing the conduction electron density. But contrary to the IPT, the MPT is applicable also at finite temperatures.

Summarizing the features of the MPT, it should be considered trustworthy for small U since it is based on perturbation theory. But furthermore it is well justified in the strong coupling regime, where the main features – the charge excitations are correctly reproduced. This is clearly one step beyond similar methods which determine the parameters a_σ and b_σ with respect to the “atomic” limit $V = 0$ ^{19,29,43}.

To calculate the susceptibility, we apply an external magnetic field B_{ext} which couples to the f - and the s -electrons. The susceptibility $\chi^{(\text{tot})}$ is given as $\frac{\partial M}{\partial B_{\text{ext}}}|_{B_{\text{ext}}=0}$, where M is the total magnetization of the system. Since the f - and s -magnetization can be computed separately, the respective contribution of the f -(s -) electrons to $\chi^{(\text{tot})}$ can be determined.

With the above-described theory, the f -electron Green function and all quantities deriveable from it can be obtained. This includes several two-particle correlation functions as e.g. the f -electron double occupancy $\langle n_\sigma^{(f)} n_{-\sigma}^{(f)} \rangle$ ^{44,45}. However, for the discussion below, we will also be interested in two-particle correlation functions which are not readily obtained from $G_{ii\sigma}^{(f)}(E)$. To determine these, as e. g. the s - f density correlation function $\langle n_\sigma^{(f)} n_{\sigma'}^{(s)} \rangle$ we need a further approximation: We construct the following effective medium Hamiltonian:

$$H^{(\text{eff})} = \sum_{\vec{k},\sigma} \epsilon(\vec{k}) s_{\vec{k},\sigma}^\dagger s_{\vec{k},\sigma} + \sum_{i,\sigma} (\epsilon_f + \Sigma_\sigma(E)) f_{i,\sigma}^\dagger f_{i,\sigma} + V \sum_{i,\sigma} (f_{i,\sigma}^\dagger s_{i,\sigma} + s_{i,\sigma}^\dagger f_{i,\sigma}) \quad (6)$$

with $\Sigma_\sigma(E)$ being the fully self-consistent solution of the DMFT-MPT scheme. Since the effective medium Hamiltonian is bilinear in fermion operators, all Green functions of interest can be evaluated exactly. By construction, the single-particle properties of model (6) are equivalent to the original model (1) solved within the DMFT-MPT scheme. Although we are aware of the fact, that using the effective Hamiltonian (6) must be seen as an approximation to the original model (1), it is in our opinion clearly one step beyond standard first-order perturbation theory for the latter, which would not reproduce the non-trivial results we will discuss below. Let us already point out here that these non-trivial results will always be accompanied by special features in quantities

which were derived from the full Hamiltonian (1) using the DMFT-MPT (e. g. the susceptibility or $\langle n_\sigma^{(f)} n_{-\sigma}^{(f)} \rangle$). They seem therefore to be not effects due to the replacement of Hamiltonian (1) with (6).

III. RESULTS AND DISCUSSION

A. The symmetric PAM

The symmetric PAM is defined by complete particle-hole symmetry, i. e. $e_f = -\frac{U}{2}$ and a particle-hole symmetric density of states of the conduction band with the chemical potential located at its center of gravity.

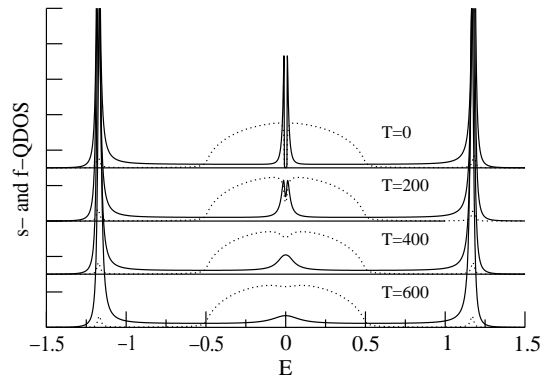


FIG. 1: s - and f -densities of states for $U = 2$, $e_f = -\frac{U}{2} = -1$, $V = 0.2$, $n^{(f)} = n^{(s)} = 1$ and various temperatures (solid line: f -DOS, dotted line: s -DOS), the temperature scale is explained in the text.

In figure 1, the s - and f -densities of states (s - and f -DOS) with $U = 2$ and $V = 0.2$ are plotted for various temperatures. The energy scale is defined by the free, i.e. unhybridized conduction band of unit width and semi-elliptic shape centered at $E = 0$. Within this energy scale, the temperatures will be given in $\frac{K}{eV}$. We have plotted the projections onto the f (s)-states using solid (dotted) lines.

The DOS consist of the charge excitations approximately located at e_f and $e_f + U$ which are dominantly of f -character and the conduction band mostly of s -character which is slightly deformed due to the hybridization. For low temperatures, an additional feature appears in the vicinity of $E = \mu = 0$, the Kondo resonance¹. It is split by the coherence gap which originates from the coherent hybridization between f - and s -states at all lattice sites.

This coherence gap might be the theoretical equivalent of the experimentally seen “pseudo-gap” e.g. in SmB_6 ⁴⁶ or in the so-called Kondo insulators, e.g. $Ce_3Bi_4Pt_3$ ⁴⁷ or $CeNiSe$ ⁴⁸. It can be understood as a level-repulsion between the conduction band states and the effective f -level located at the chemical potential. Since this effective f -

level is clearly correlation-induced, the coherence gap is as well.

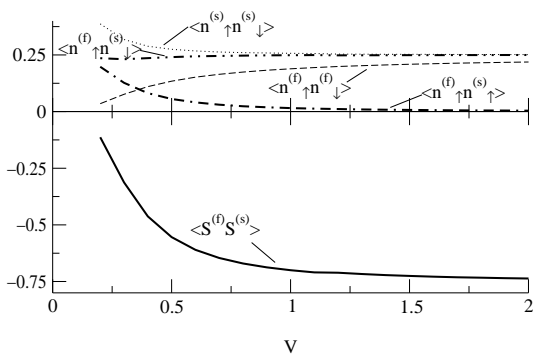


FIG. 2: The on-site double-occupancy correlation functions and the local spin-spin correlation function ($\vec{S}_i^{(f)} \vec{S}_i^{(s)}$) as function of the hybridization strength V for $T = 0$ (other parameters as in fig. 1)

The DOS obtained by our method compare very well with those calculated by QMC in $d = 1^{6,7}$, $d = 2^8$ and $d = \infty^{3,19}$. At least for $d = 1$ and $d = 2$, there is one qualitative difference, however. In the MPT, the Kondo resonance is of pure f -character, whereas in the cited papers, the conduction band also contributes to the resonance. Whether this is due to the maximum-entropy method⁴⁹ necessary to complement the QMC formalism, or an artefact of our method, remains an open question. However, physically relevant is only the total density of states (f plus conduction band). The choice of projecting the DOS onto the f - and s -states, i.e. onto the basis given by the $V = 0$ solution of the problem is rather arbitrary. Therefore, the above-discussed differences seem to be of minor importance.

Focusing on the Kondo screening problem, the question arises on how one can observe it. One possibility found in the literature is the definition of an effective magnetic moment $T\chi(T)$. This is motivated by the Curie law which, however, only holds for high temperatures. In the SIAM, there is a suppression of $T\chi(T)$ coinciding with the temperature scale T_K which also governs the other low-energy properties of the system. In analogy to the SIAM, the behaviour of $T\chi(T)$ is often interpreted as indirect indicator for the onset of Kondo screening in the PAM^{3,4}. Another criterion of Kondo screening, which we will focus on, might be found in spin-spin correlation functions. Let us look for example at the problem of two $S = \frac{1}{2}$ spins. Of the four possible states of this system, three are of triplet and one is of singlet nature. The spin-spin correlation function takes the value $\langle \vec{S}_a \vec{S}_b \rangle = \frac{1}{4}$ for the triplet states and $\langle \vec{S}_a \vec{S}_b \rangle = -\frac{3}{4}$ for the singlet state (a and b denote the two spins). In the following, we will discuss only the on-site interband spin-spin correlation function $\langle \vec{S}_i^{(f)} \vec{S}_i^{(s)} \rangle$. It is obvious that this function can be an indicator only for local singlet formation, as will be discussed in more detail below.

In figure 2, the on-site interband spin-spin correlation function $\langle \vec{S}_i^{(f)} \vec{S}_i^{(s)} \rangle$ as well as several on-site double occupancy correlation functions are plotted as function of the hybridization strength V for $T = 0$ (other parameters as in figure 1). With increasing V , the on-site spin-spin correlation function approaches the value $-\frac{3}{4}$. In the same range of V , the interband double occupancy with parallel spin, $\langle n_{i\sigma}^{(f)} n_{i\sigma}^{(s)} \rangle$ vanishes, whereas the respective correlation function with opposite spin indices, $\langle n_{i\sigma}^{(f)} n_{i-\sigma}^{(s)} \rangle$ stays almost constant. In analogy to the two-spin problem, these are clear indications of a local singlet correlation. A similar transition in the spin-spin correlation function has been seen in a PAM with next-neighbor hybridization using QMC, where it has been interpreted as singlet formation⁹.

In the upper graphs of figures 3 and 4, the correlation functions of figure 2 are plotted as function of temperature for large ($V = 0.6$) and small ($V = 0.2$) hybridization strengths. Additionally, the lower graphs show the respective susceptibilities. In the large- V case, the above described transition in the various correlation functions is clearly visible: $\langle \vec{S}_i^{(f)} \vec{S}_i^{(s)} \rangle \rightarrow -\frac{3}{4}$ and $\langle n_{i\sigma}^{(f)} n_{i\sigma}^{(s)} \rangle$ shows a huge drop around $T \approx 3000$, being of very small value at low temperatures. In the same temperature range, the susceptibility vanishes. Both the f - and s -contribution to $\chi^{(tot)}$ disappear simultaneously. From these findings, we propose the occurrence of *local Kondo singlet* formation. With the term local Kondo singlet (LKS), we want to stress, that the singlet formation is predominantly a local process determined by the binding of one f - and one

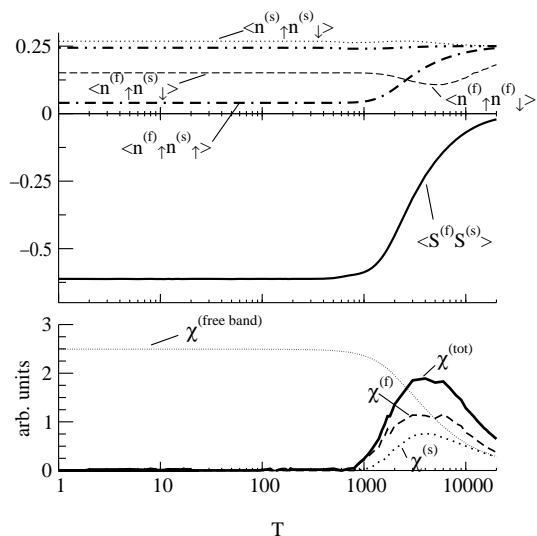


FIG. 3: Upper panel: the correlation functions of figure 2, but as function of temperature for $V = 0.6$. Lower panel: the susceptibility $\chi^{(tot)}$ as well as the f - and s -contribution to $\chi^{(tot)}$ are plotted. The thin dotted line ($\chi^{(free\ band)}$) shows the susceptibility of a free, i.e. unhybridized and uncorrelated conduction band with same parameters as the s -band used in the other calculations.

s -electron at each lattice site. In the opposite case of collective Kondo screening as it could occur for small V , the local correlation functions discussed here need not show any particularities. Our proposal is further supported by the behavior of the conduction band double occupancy $\langle n_{i\sigma}^{(s)} n_{i-\sigma}^{(s)} \rangle$. In the large- V region, where we propose the LKS formation, this correlation function is reduced compared to the small- V case, as can be clearly seen in figure 2. This indicates a tendency towards localization of the conduction electrons, which is exactly what one would expect in the case of LKS formation. The unique temperature scale which we identify with the Kondo temperature of $T_K \approx 1000K$ seems to be very large. This cannot be due to the ‘‘Hartree-Fock-character’’ implied by the simple effective medium approach of equation (6) used to determine the higher correlation functions, since the same temperature scale appears in the susceptibility, which is determined from the full Hamiltonian (equation (1)) in the DMFT-MPT scheme. Whether T_K is over-estimated due to the mean-field character of the DMFT or the use of the MPT, or whether it displays the true behavior of the system, would be speculation. However, comparing our method with other means of calculation (e.g. numerical renormalization group calculations (NRG)^{20,50}), the DMFT-MPT seems to overestimate energy scales. We believe this is connected to the fact that the MPT, as any perturbative method, is unable to reproduce the exponential temperature scale typical for the Kondo physics³². A detailed comparison with complementary methods, e.g. NRG, is needed to shed further light on this.

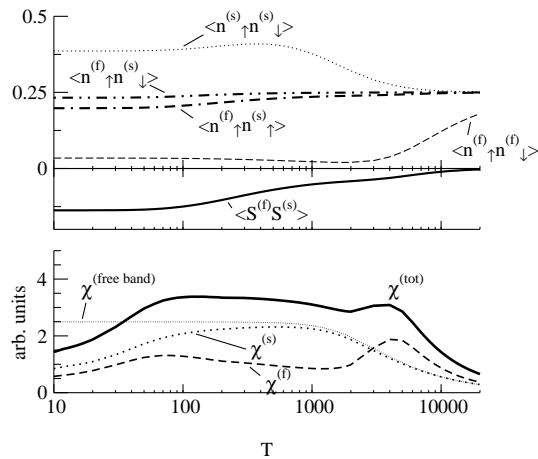


FIG. 4: As figure 3, but with small $V = 0.2$

For small V (figure 4), the situation is completely different. The systems with small and large V behave similar only for very low and very high temperatures. For very high temperatures, a Curie-like behavior is found as expected. For $T = 0$, the susceptibility vanishes also in the small- V case. This is compatible with the exact result by Tsunetsugu et al.², who proved the singlet nature of the ground state of the symmetric PAM independent of the size of V and showed the existence of

a spin gap. However, for small hybridization the various correlation functions discussed above show none of the occurrences which led us to the conclusion of the local Kondo singlet formation in the large- V case. The susceptibility shows two features. The one at the high temperature $T_{high} \approx 4000K$ corresponds to the delocalization of the f -electrons due to thermal excitations. As can be seen at the decomposition of $\chi^{(tot)}$, only the f -contribution is responsible for this feature. The conduction electron contribution $\chi^{(s)}$ resembles at and below T_{high} still the susceptibility of a system of uncorrelated electrons ($\chi_{free\ band}$). The delocalization of the f -electrons is visible in the increase of $\langle n_{i\sigma}^{(f)} n_{i-\sigma}^{(f)} \rangle$ for $T > T_{high}$. The Kondo screening sets in at the much lower Kondo temperature $T_K \approx 100K$. This corresponds to the temperature where the Kondo resonance appears in the DOS (see figure 1). As already mentioned, the local correlation functions show here only a weak signature of Kondo screening. The Kondo screening for small V is a collective effect, the quantities accessible by our theory do not allow more detailed investigation of this state.

To summarize the discussion of the symmetric PAM, we find two different kinds of Kondo singlet formation depending on the hybridization strength. Where for small V the singlet formation involves non-local or collective screening of the f -electrons by the conduction band electrons, in the large V domain, the singlet formation is dominantly a local process. At every lattice site, one f - and one s -electron couple to form a local Kondo singlet (LKS).

B. Exhaustion problem

One important question concerning the screening behavior is that of exhaustion: What happens if the number of conduction electrons $n^{(s)}$ is reduced (the number of f -electrons is fixed $n^{(f)} = 1$)? This question was recently brought into attention by Nozières²⁴. In this section, we want to present our results concerning ‘‘exhaustion’’.

In figure 5, the f -electron density of states (f -DOS) is plotted for $T = 0$ and various $n^{(s)}$. The main change in the f -DOS is the shift of the charge excitations as well as the Kondo resonance towards lower energies. The shift of the charge excitations is due to an adjustment of e_f which is necessary to keep the constraint $n^{(f)} = 1$ with decreasing $n^{(s)}$. The Kondo resonance also moves towards lower energies as its position is pinned to the chemical potential μ . The coherence gap stays in the vicinity of μ , too. However, the relative position of the gap, the Kondo peak and μ changes. Whereas for $n^{(s)} = 1$, the Kondo resonance and the gap are centered symmetrically around μ , for $n^{(s)} < 1$ the situation becomes asymmetric. The chemical potential moves into the lower half of the resonance. As a direct consequence, the shape of the resonance becomes asymmetric. This strongly resembles the behavior found for the SIAM^{1,32}. The relative shift of μ and the Kondo resonance has also an impor-

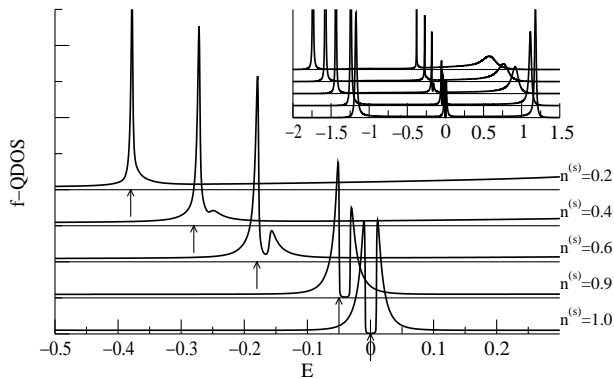


FIG. 5: f -densities of states for $T = 0$ in the vicinity of the chemical potential (arrows). The system parameters are as in figure 1 but the conduction band occupation is varied from $n^{(s)} = 1$ to $n^{(s)} = 0.2$ as indicated. The inset shows the f -DOS over the full energy range

tant consequence for the coherence gap. For $n^{(s)} < 1$ the system is metallic since μ is no longer located within the gap. With decreasing $n^{(s)}$, the gap moves further away from the chemical potential. The imaginary part of the self-energy $\Im\Sigma_{\sigma}(E)$ at the gap increases thereby since it shows a “Fermi-liquid” E^2 dependence around $E = \mu$. For $n^{(s)}$ slightly below unity, the gap is still present in form of a “pseudo-gap”. However, for $n^{(s)}$ approaching zero, the gap closes completely.

This resembles the behavior found in $Ce_3Bi_4Pt_3$ upon doping with lanthanum⁴⁷. The undoped system is an insulator with a very small gap believed to be a prototypical Kondo insulator. On doping La , the system becomes a metallic heavy-fermion system. In reference 47 this is interpreted as due to the de-construction of lattice coherence by disorder. From the behavior of the PAM, one might also conclude that simply the change of the electron density due to doping would also be sufficient to explain this metal-insulator transition.

In figure 5 a broadening of the upper charge excitation is observed for $n^{(s)} \rightarrow 0.2$. Here, the upper charge excitation overlaps with the conduction band which results in a stronger hybridization. This could be prevented by using a larger value for U . However, the impact of this on the results discussed below is negligible.

Let us now turn to the actual problem of exhaustion. In the case of the symmetric PAM ($n^{(s)} = n^{(f)} = 1$), we have found a singlet ground state with a finite spin gap which is in agreement with QMC results⁵¹ and exact statements concerning the ground state². It is not clear how the system will react when the number of conduction electrons is reduced while $n^{(f)} = 1$ is kept constant. One possibility would be a partial or complete breakdown of the screening since the conduction-band filling is not sufficient to screen the magnetic moments of all f -electrons. However, conduction-band mediated f - f correlations could again lead to a singlet ground state via intersite singlet correlations. This scenario has been

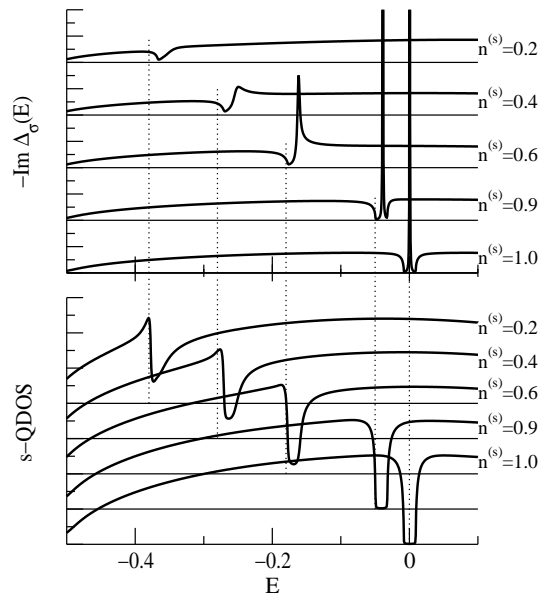


FIG. 6: s -DOS and imaginary part of the hybridization function $-\Im\Delta_{\sigma}(E)$ close to the chemical potential μ for the same parameters as in figure 5. The dotted line indicates the position of μ for the respective value of $n^{(s)}$. The curves for $n^{(s)} \neq 1$ have been shifted vertically for clarity.

confirmed for the two-impurity Kondo problem⁵².

Recently, the exhaustion problem has been discussed as the origin of a new low-energy scale^{4,5,19,20,24,53}. In one of these publications¹⁹, the iterated perturbation theory has been applied, which is very similar to the approximations used in this paper. There, the authors found a gap close to the chemical potential in the effective hybridization defined by $-\Im\Delta_{\sigma}(E)$ (see equation (2)). In figure 6, $-\Im\Delta_{\sigma}(E)$ as well as the conduction band density of states (s -DOS) are plotted in the vicinity of μ for various conduction band fillings. The parameters correspond to the DOS plotted in figure 5. In the s -DOS, the coherence gap but no Kondo resonance is visible. The latter appears only in the projection onto f -states (f -DOS) and is therefore of pure f -character. Again, the coherence gap shifts together with μ towards lower energies on reducing $n^{(s)}$. Let us focus on $-\Im\Delta_{\sigma}(E)$, the upper picture in figure 6. Independently of $n^{(s)}$ there exists a gap/dip close to the chemical potential. However, in the symmetric case ($n^{(s)} = 1$) a sharp δ -like peak appears exactly at $E = \mu$. So $-\Im\Delta_{\sigma}(E = \mu)$ is large in the symmetric case, but already for any small change in $n^{(s)}$, $-\Im\Delta_{\sigma}(E = \mu)$ becomes small since μ lies within the gap or dip. In reference 19, the authors interpret the dip which they find for $n^{(s)} = 0.4$ in the effective hybridization as sign of the exhaustion of the conduction electrons. However, this reduction of $-\Im\Delta_{\sigma}(E)$ around $E = \mu$, which we also find for $n^{(s)} = 0.4$, continuously develops into a gap for $n^{(s)} = 0.9$. In the interpretation of the cited work, this would imply that the exhaustion

problem is stronger for $n^{(s)} \rightarrow 1$ than for $n^{(s)} = 0.4$ since the dip evolves into a true gap. The special case $n^{(s)} = 1$ with its “preformed gap” surrounding the δ -like peak in $-\Im\Delta_\sigma(E)$ would also need further considerations. In our opinion, without clearer justification, this gap/dip cannot be taken as a direct sign of exhaustion.

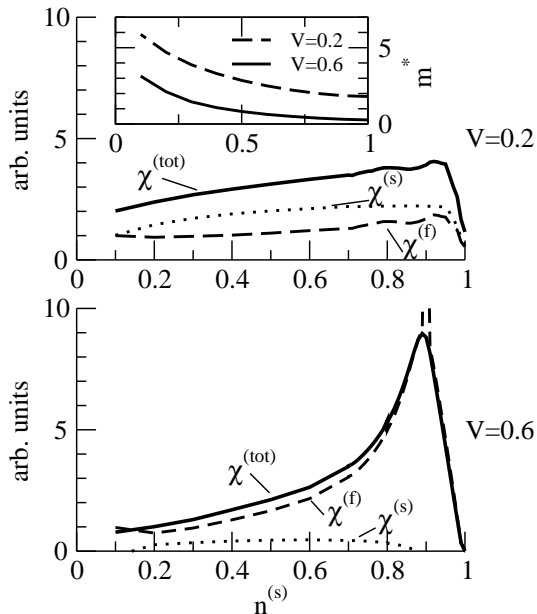


FIG. 7: The $T = 0$ -susceptibility and its respective f -level and conduction band contributions for small $V = 0.2$ (upper panel) and large $V = 0.6$ (lower panel) as function of conduction band fillig. In the inset of the upper panel, the effective mass is plotted for both values of V . The remaining parameters are as in figure 2.

In figure 7, we have plotted the zero-temperature susceptibility for small $V = 0.2$ and large $V = 0.6$ as function of the conduction band occupation number $n^{(s)}$. In addition to that, the effective mass $m^* = 1 - \frac{\partial \Sigma}{\partial E}|_{E=0}$ is plotted in the inset of the upper panel.

From these figures, one gains some insight in the stability of the LKS in case of exhaustion ($n^{(s)} < n^{(f)} = 1$). In the small- V case, $\chi^{(tot)}$ is roughly proportional to the value of the DOS at $E = \mu$ for less than half-filled conduction band. Both the f - and s -electrons contribute to $\chi^{(tot)}$. Contrary to that, for the LKS-dominated system ($V = 0.6$), only the f -electrons react to an external field. The conduction band contribution $\chi^{(s)}$ is negligible for $n^{(s)} < 0.9$. So we conclude that all conduction electrons are more or less bound into LKS states and therefore unable to react to an external magnetic field. Another hint can be derived from the fact that $\langle \vec{S}_i^{(f)} \vec{S}_i^{(s)} \rangle$ decreases linearly with $n^{(s)}$ (not plotted). This can be interpreted as a linear decrease of the number of LKS. I.e. all available conduction electrons form a LKS, and $n^{(bach)} = 1 - n^{(s)}$ f -electrons remain unpaired. These are the equivalent of the “bachelor spins” discussed by Nozières for the Kondo lattice model²⁴. Following his argumentation, they can

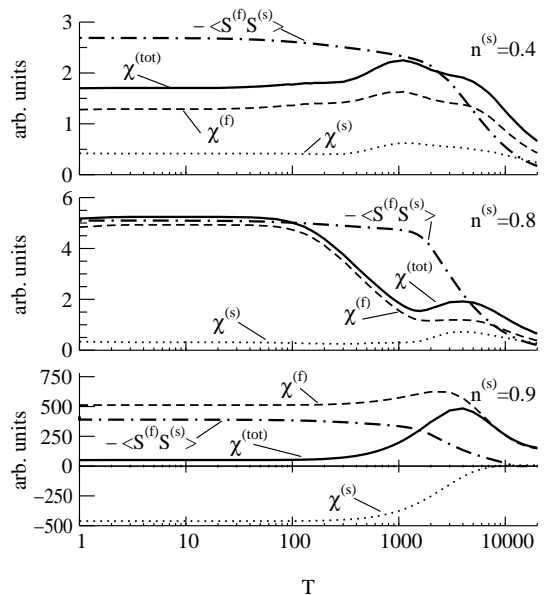


FIG. 8: The susceptibility, its f - and s -contributions and the on-site interband spin-spin correlation function $\langle \vec{S}_i^{(f)} \vec{S}_i^{(s)} \rangle$ as function of temperature for three different conduction band occupations $n^{(s)} \in \{0.9, 0.8, 0.4\}$. The hybridization strength is $V = 0.6$, the data corresponds to figure 7. Please note that we have plotted the negative of $\langle \vec{S}_i^{(f)} \vec{S}_i^{(s)} \rangle$ and rescaled it by a factor 10 for the upper two, and a factor 1000 for the lower plot.

be described as a system of $n^{(bach)}$ spin- $\frac{1}{2}$ fermions. In the KLM these are “hard-core”-fermions since for the localized spins, double occupancy is strictly forbidden. In our case of the PAM, double occupancy is principally possible, only suppressed by the on-site repulsion U . Therefore, these bachelor fermions should show similarities to a non-degenerate Hubbard model with finite U . One feature of the Hubbard model is the Mott-Hubbard transition^{28,54}. For an exactly half-filled system with sufficiently large U , the otherwise metallic system becomes insulating due to the electron correlations. Approaching the half-filled situation from lower carrier concentrations, the effective mass strongly increases, and diverges at half-filling. Bearing this in mind, the behavior of the effective mass shown in the inset of figure 7 can be understood. The most prominent feature is the increase of m^* for $n^{(s)} \rightarrow 0$. The latter, however, implies that the above-discussed bachelor-fermion model approaches half-filling, since the number of unpaired f -electrons goes to unity. In terms of this model, the system is in the proximity of the Mott-Hubbard transition. Please note, that in the PAM with finite hybridization, $n^{(s)} = 0$ is only possible for extreme parameter conditions, namely $e_f \rightarrow -\infty$ and $U \rightarrow \infty$. Our method is not feasible for these parameters.

Let us now discuss why the susceptibility is enlarged at $n^{(s)} = 0.9$. Looking at the partial contributions $\chi^{(f)}$ and $\chi^{(s)}$ at $n^{(s)} = 0.9$, we note that both take on large values.

However, while $\chi^{(f)}$ is positive, the conduction band contribution becomes negative (see lowest panel of figure 8). We believe this is due to the proximity of a magnetically ordered phase. Since we do not allow for antiferromagnetic ordering in our method, we obtain a paramagnetic system for the shown parameters. For larger values of U , however, we also see an onset of ferromagnetic order. The critical U_c is lower for $n^{(s)} \approx 0.9$ than for other values of $n^{(s)}$. So the peak in the susceptibility is in our opinion due to the proximity of the ferromagnetic phase. The opposite signs of $\chi^{(f)}$ and $\chi^{(s)}$ result from the fact that in the ferromagnetic phase, the conduction band will be polarized antiparallel to the f -levels, as will be shown in a forthcoming publication. However, using quantum Monte Carlo methods, antiferromagnetic order was found for $n^{(s)} \rightarrow 1^4$. In principle, the investigation of an antiferromagnetic order is also possible within our method and is planned for future studies. The results of reference 4 suggest that for $n^{(f)} = 1$ and $n^{(s)} \rightarrow 1$ the antiferromagnetic phase will be stable against the ferromagnetic phase.

Note that also in the weakly hybridized case, this increase in m^* is visible. This is similar to the findings in reference 20 and can be understood in a similar fashion as in the large- V case (a detailed discussion is given in reference 5).

In figure 8, the temperature dependence of the susceptibility and the on-site interband spin-spin correlation function is plotted for $V = 0.6$ and $n^{(s)} \in \{0.4, 0.8, 0.9\}$. As can be seen, the temperature where the LKS formation occurs, is nearly independent of $n^{(s)}$. The LKS formation should not be confused with the potential new low-energy scale discussed in recent publications^{5,20}. In our results, the only possible indication for this energy scale could be the increase of m^* . Complementary methods such as numerical renormalization theory^{1,20,50} should be used to get more insight at this question.

IV. CONCLUSIONS

In the present work, we have studied the periodic Anderson model (PAM) using the modified perturbation theory in the context of the dynamical mean-field theory. This approach is well motivated both for the large and small coupling regime. Furthermore, applying it to the single-impurity Anderson model³² and the Hubbard

model^{30,31,38} good accordance with (numerically) exact methods has been found. Being fast and numerically stable, all parameter regions of the model can conveniently be investigated, this includes $T = 0$ as well as finite temperatures.

The density of states generally consists of the charge excitations of the localized level, the conduction band structure and, for low temperatures, an additional peak, the Kondo resonance. At least for symmetric parameters the latter is split by the coherence gap. The Kondo resonance is ascribed to the phenomenon of Kondo screening meaning the quenching of the magnetic moment of the localized levels by the conduction electrons.

In the case of the symmetric PAM, where the f -level and the conduction band are both half-filled and the two charge excitations lie symmetrically around the chemical potential, the ground state is always a singlet with a spin gap which is in accordance with the assumption of complete Kondo screening. Investigating several on-site correlation functions and the susceptibility as function of the hybridization strength V , we see a crossover between two qualitatively different regions. Whereas for small V , the Kondo screening is a collective effect, for intermediate and large V , the screening is a dominantly local process. At each lattice site a *local Kondo singlet* exists. It is built up by one conduction- and one f -electron spin.

On reducing the number of conduction electrons, the LKS remain stable. However, due to unavailability of s -electrons, a finite number of f -electrons are unpaired (bachelor fermions). Following a recent reasoning by Nozières²⁴ and others⁵, the low-temperature physics of the system should be describable by an effective model which only regards these bachelor fermions. Our results are compatible with this proposal. In the susceptibility, we found indications of the proximity of magnetically ordered phases. These will be subject of a forthcoming paper.

Acknowledgments

We wish to thank M. Pottthoff for many helpful discussions. Financial support by the Volkswagen foundation is gratefully acknowledged. One of the authors (D. M.) would like to thank the Friedrich-Naumann foundation for support this work.

* Dietrich.Meyer@physik.hu-berlin.de

¹ A. C. Hewson, *The Kondo Problem to Heavy Fermions* (Cambridge University Press, 1993).

² H. Tsunetsugu, M. Sigrist, and K. Ueda, *Rev. Mod. Phys.* **69**(3), 809 (1997).

³ M. Jarrell, *Phys. Rev. B* **51**(12), 7429 (1995).

⁴ A. Tahvildar-Zadeh, M. Jarrell, and J. Freericks, *Phys. Rev. B* **55**(6), R3332 (1997).

⁵ A. Tahvildar-Zadeh, M. Jarrell, and J. Freericks, *Phys. Rev. Lett.* **80**(23), 5168 (1998).

⁶ C. Gröber and R. Eder, *Phys. Rev. B* **57**(20), R12659 (1998).

⁷ C. Gröber and R. Eder, *Phys. Rev. B* **59**(16), 10405 (1999).

⁸ C. Gröber and R. Eder, *Excitation spectra of the two dimensional kondo insulator*, cond-mat/9909008.

⁹ C. Huscroft, A. K. McMahan, and R. T. Scalettar, *Phys.*

- Rev. Lett. **82**(11), 2342 (1999).
- ¹⁰ H. Leder and B. Mühlischlegel, Z. Phys. B **29**, 341 (1978).
 - ¹¹ H. Schweitzer and G. Czycholl, Solid State Commun. **74**(8), 735 (1990).
 - ¹² H. Schweitzer and G. Czycholl, Z. Phys. B **79**, 377 (1990).
 - ¹³ R. Doradziński and J. Spalek, Phys. Rev. B **56**(22), R14239 (1997).
 - ¹⁴ R. Citro and J. Spalek, Physica B **230**, 469 (1997).
 - ¹⁵ R. Doradziński and J. Spalek, Phys. Rev. B **58**(6), 3293 (1998).
 - ¹⁶ B. Möller and P. Wölfle, Phys. Rev. B **48**(14), 10320 (1993).
 - ¹⁷ T. V. Rao, G. G. Reddy, and A. Ramakanth, Solid State Commun. **81**(9), 795 (1992).
 - ¹⁸ T. V. Rao, G. G. Reddy, and A. Ramakanth, J. Phys. Chem. Solids **55**(2), 175 (1994).
 - ¹⁹ N. S. Vidhyadhiraja, A. N. Tahvildar-Zadeh, M. Jarrell, and H. R. Krishnamurthy, preprint pp. cond-mat/9905408 (1999).
 - ²⁰ T. Pruschke, R. Bulla, and M. Jarrell, preprint p. to appear in Physica B (1999).
 - ²¹ D. Meyer, W. Nolting, G. Reddy, and A. Ramakanth, phys. stat. sol. (b) **208**, 473 (1998).
 - ²² D. Meyer and W. Nolting, Physica B **259**, 918 (1999).
 - ²³ D. Meyer and W. Nolting, *Periodic anderson model: Magnetic properties*, to appear in Physica B.
 - ²⁴ P. Nozières, Eur. Phys. J. B **6**, 447 (1998).
 - ²⁵ J. R. Schrieffer and P. A. Wolff, Phys. Rev. **149**(2), 491 (1966).
 - ²⁶ W. Metzner and D. Vollhardt, Phys. Rev. Lett. **62**, 324 (1989).
 - ²⁷ T. Pruschke, M. Jarrell, and J. K. Freericks, Adv. Phys. **44**(2), 187 (1995).
 - ²⁸ A. Georges, G. Kotliar, W. Krauth, and M. J. Rozenberg, Rev. Mod. Phys. **68**(1), 13 (1996).
 - ²⁹ H. Kajueter and G. Kotliar, Phys. Rev. Lett. **77**(1), 131 (1996).
 - ³⁰ M. Potthoff, T. Wegner, and W. Nolting, Phys. Rev. B **55**(24), 16132 (1997).
 - ³¹ T. Wegner, M. Potthoff, and W. Nolting, Phys. Rev. B **57**(11), 6211 (1998).
 - ³² D. Meyer, T. Wegner, M. Potthoff, and W. Nolting, Physica B **270**, 225 (1999).
 - ³³ E. Müller-Hartmann, Z. Phys. B **74**, 507 (1989).
 - ³⁴ H. Schweizer and G. Czycholl, Solid State Commun. **69**(2), 171 (1989).
 - ³⁵ A. Martin-Rodero, F. Flores, M. Baldo, and R. Pucci, Solid State Commun. **44**, 911 (1982).
 - ³⁶ K. Yamada, Prog. Theo. Phys. **53**, 970 (1975).
 - ³⁷ V. Zlatič and B. Horvatič, Phys. Rev. B **28**(12), 6904 (1983).
 - ³⁸ M. Potthoff, T. Herrmann, T. Wegner, and W. Nolting, phys. stat. sol. (b) **210**, 199 (1998).
 - ³⁹ A. Harris and R. Lange, Phys. Rev. **157**(2), 295 (1967).
 - ⁴⁰ J. M. Luttinger and J. C. Ward, Phys. Rev. **118**(5), 1417 (1960).
 - ⁴¹ J. Friedel, Can. J. Phys. **34**, 1190 (1956).
 - ⁴² D. Langreth, Phys. Rev. **150**(2), 516 (1966).
 - ⁴³ O. Takagi and T. Saso, preprint pp. cond-mat/9907409 (1999).
 - ⁴⁴ W. Nolting, *Viel-Teilchen-Theorie*, vol. 7 of *Grundkurs: Theoretische Physik* (Friedr. Vieweg & Sohn Verlagsgesellschaft mbH, Braunschweig/Wiesbaden, 1997), 3rd ed.
 - ⁴⁵ T. Herrmann, *Korrelationseffekte in der elektronischen Struktur eines Modell-Bandmagneten*, Master's thesis, Humboldt-Universität zu Berlin (Mar. 1996).
 - ⁴⁶ J. W. Allen, B. Batlogg, and P. Wachter, Phys. Rev. B **20**(12), 4807 (1979).
 - ⁴⁷ M. F. Hundley, P. C. Canfield, J. D. Thompson, Z. Fisk, and J. M. Lawrence, Phys. Rev. B **42**(10), 6842 (1990).
 - ⁴⁸ C. N. Davydov, S. Kambe, A. G. M. Jansen, P. Wyder, N. Wilson, G. Lapertot, and J. Flouquet, Phys. Rev. B **55**(12), R7299 (1997).
 - ⁴⁹ M. Jarrell and J. E. Gubernatis, Phys. Rep. **269**(3), 133 (1995).
 - ⁵⁰ R. Bulla, A. C. Hewson, and T. Pruschke, J. Phys.: Condens. Matter **10**, 8365 (1998).
 - ⁵¹ R. Blankenbecler, J. R. Fulco, W. Gill, and D. J. Scalapino, Phys. Rev. Lett. **58**(4), 411 (1987).
 - ⁵² I. Affleck, A. W. W. Ludwig, and B. A. Jones, Phys. Rev. B **52**(13), 9528 (1995).
 - ⁵³ A. Tahvildar-Zadeh, M. Jarrell, T. Pruschke, and J. Freericks, Phys. Rev. B **60**(15), 10782 (1999).
 - ⁵⁴ F. Gebhard, *The Mott Metal-Insulator Transition - Models and Methods*, vol. 137 of *Springer Tracts in Modern Physics* (Springer, Heidelberg, 1997).